Zeolites

DOI: 10.1002/anie.201309426

Cobalt Imidazolate Metal–Organic Frameworks Photosplit CO_2 under Mild Reaction Conditions**

*Sibo Wang, Wangshu Yao, Jinliang Lin, Zhengxin Ding, and Xinchen Wang**

Abstract: *Metal–organic frameworks (MOFs) have shown great promise for CO_2 capture and storage. However, the operation of chemical redox functions of framework substances and organic CO_2-trapping entities which are spatially linked together to catalyze CO_2 conversion has had much less attention. Reported herein is a cobalt-containing zeolitic imidazolate framework (Co-ZIF-9) which serves as a robust MOF cocatalyst to reduce CO_2 by cooperating with a ruthenium-based photosensitizer. The catalytic turnover number of Co-ZIF-9 was about 450 within 2.5 hours under mild reaction conditions, while still keeping its original reactivity during prolonged operation.*

The conversion of CO_2 into chemical feedstocks has attracted enormous attention owing to the increasing concern with global energy and environmental problems.[1] The light-stimulated CO_2 conversion promises the utilization of solar energy to fulfill a vital mission of artificial photosynthesis, which usually exploits dyes, semiconductors, electron mediators, and desirable coupling to CO_2 activators.[2] A great deal of effort has therefore been devoted to developing light harvesters, electron-transport carriers, CO_2 activators, and their integration into a chemical system for CO_2 reduction.[3]

Transition-metal ions of multiple redox states and organic ligands are indispensable for creating electron-transport chains, which cooperate with light harvesters and CO_2 activators, to accelerate the multielectron reduction of CO_2 coupled to a proton flux so as to avoid the formation of high-energy intermediates. Cobalt, nickel, and copper ions/complexes have been demonstrated to act as cocatalysts by promoting the kinetics of both charge-separation and surface reaction for CO_2 photoreduction.[4]

The search for CO_2 activators has recently experienced an intense exploration into organocatalysts as coordination substrates for the capture and activation of CO_2 to facilitate CO_2 reduction with stoichiometic reductants.[5] Among various organocatalysts, imidazolate-based ionic liquids[6] have been shown to not only have high adsorptive capabilities for CO_2 but also have a stabilizing effect on the CO_2^- by complexation.[7] The stabilizing effect of the organic imidazolium motifs on CO_2^- greatly reduces the overall barrier to the CO_2 reduction reaction because the formation of the CO_2^- intermediate is the first step of CO_2 conversion which has a very high energy of activation, thus establishing a rate-limiting step.[8] Imidazolate-based ionic liquids are also considered to be precursors for N-heterocyclic carbenes (NHCs)[9] through deprotonation at the C2 position, and the NHCs thus formed have been employed to activate and convert CO_2 into methanol by a deoxygenative transformation pathway.[10]

The merging of organic CO_2 activators with transition-metal catalysis for carbon fixation chemistry is therefore desired, but it is still in its infancy. This new field motivated the material design of transition-metal ions with imidazolate-based linkers in a metal–organic framework. That way, multifunctional porous scaffolds can be rationally designed and developed for the capture, activation, and conversion of CO_2 in a one-pot fashion. When carefully coupled to an appropriate photocatalyst, an artificial photosynthesis system might be realized.

MOFs[11] are constructed by metal ions and organic linkers, and are an intriguing class of microporous crystalline materials with flexible tunability in composition, structure, and functionality for gas storage,[12] separation,[13] catalysis,[14] chemical sensing,[15] ion exchange,[16] and drug delivery.[17] Zeolitic imidazolate frameworks (ZIFs)[18] are a subclass of MOFs and possess high chemical and thermal stabilities[19] with great potential for CO_2 capture.[20] Metal imidazolate MOFs have indeed been employed as precursors of solid carbenelike catalysts for organosynthesis.[21] Nevertheless, to the best of our knowledge, there is no report on the applications of MOFs as cocatalysts for photochemical reduction of CO_2. Herein, we report a cobalt-containing benzimidazolate MOF (termed as Co-ZIF-9) as a microporous cocatalyst to promote the capture, concentration, and conversion of CO_2 into CO with light.

The Co-ZIF-9 was synthesized according to the reported procedures.[19] Both single-crystal X-ray diffraction (XRD) (see Table S1 in the Supporting Information) and power XRD (see Figure S1) analyses revealed that the crystal structure of Co-ZIF-9 was successfully achieved, consistent with the literature.[19] As shown in Figure 1, Co-ZIF-9 adopts a microporous crystalline structure composed of cobalt(II) ions linked to benzimidazolate (bIm) ligands.

[*] S. Wang, W. Yao, J. Lin, Prof. Z. Ding, Prof. X. Wang
State Key Laboratory of Photocatalysis on Energy and Environment, and College of Chemistry and Chemical Engineering
Fuzhou University
Fuzhou 350002 (China)
E-mail: xcwang@fzu.edu.cn
Homepage: http://wanglab.fzu.edu.cn

[**] Supported by the National Basic Research Program of China (2013CB632405 and 2014CB239303), the National Natural Science Foundation of China (21033003 and 21273039), the State Key Laboratory of NBC Protection for Civilian (SKLNBC2013-04K), and the Specialized Research Fund for the Doctoral Program of Higher Education (20133514110003).

Supporting information for this article is available on the WWW under http://dx.doi.org/10.1002/anie.201309426.

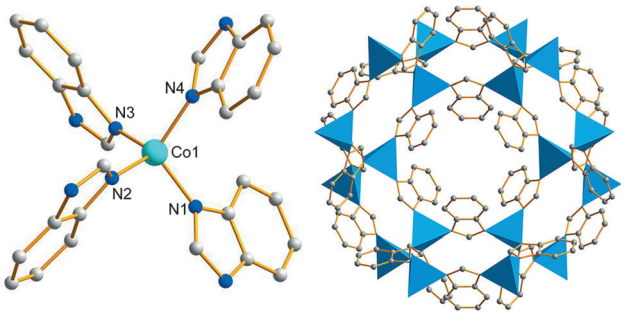

Figure 1. Chemical structure of Co-ZIF-9. Ball-and-stick representation of the second building units showing the coordination environment around cobalt (left). Packing diagram of Co-ZIF-9 (right). Hydrogen atoms are omitted for clarity. Co light blue, C gray, N blue.

Tetrahedral cobalt is solely coordinated by N atoms in the 1,3-positions of the bIm bridging ligands with a Co-bIm-Co angle of 145°, thus creating a porous framework. Comparison between the fourier transform infrared spectroscopy (FTIR) spectra of Co-ZIF-9 and benzimidazole revealed a significant difference (see Figure S2). A strong and broad band (2200–3400 cm^{-1}) with the maximum at about 2800 cm^{-1}, corresponding to the N-H···N hydrogen bond, was observed for benzimidazole, whereas for the Co-ZIF-9 the disappearance of those absorption bands revealed that the benzimidazole linkers were fully deprotonated during the formation of the Co-ZIF-9 structure.[22] The stability of the synthesized Co-ZIF-9 was first examined by thermal analysis, thus showing a high thermal stability of up to 500 °C (see Figure S3). Obviously, the Co-ZIF-9 features both cobalt(II) and imidazolate-based functionalities in a defined chemical environment.

The CO_2 reduction reactions were conducted in a visible-light-driven catalytic system using $[Ru(bpy)_3]Cl_2 \cdot 6H_2O$ (bpy = 2′2-bipyridine) and Co-ZIF-9 as a photosensitizer and a cocatalyst, respectively, along with triethanolamine (TEOA) as an electron donor, under mild reaction conditions (20 °C and 1 atm CO_2).

We first conducted a series of reference experiments. As can be seen in Table 1, in the dark there was no gas detected in the system. Upon visible-light illumination, CO_2 was split into CO at a reaction rate of 1.4 μmol min^{-1}, along with the evolution of H_2 with a rate of 1.0 μmol min^{-1} (entry 1). These results underline the involvement of the dye-excited state in the catalytic reaction, as further confirmed by the fact that no reaction occurred when the dye was absent (entry 3). The mixture of CO and H_2 is the main component of syngas, which is chemical feedstock in the Fischer–Tropsch process to produce liquid fuels.[23]

Table 1: The research of reaction conditions.[a]

Entry	CO [μmol]	H_2 [μmol]	H_2+CO [μmol]	TON[b]
1	41.8	29.9	71.7	89.6
2[c]	n.d.[d]	n.d.	–	–
3[e]	n.d.	n.d.	–	–
4[f]	n.d.	n.d.	–	–
5[g]	1.2	1.8	3.0	3.8
6[h]	28.1	17.6	45.7	57.1
7[i]	3.7	2.4	6.1	7.6
8[j]	n.d.	1.0	1.0	1.2
9[k]	n.d.	n.d.	–	–

[a] Reaction conditions: $[Ru(bpy)_3]Cl_2 \cdot 6H_2O$ (10.0 μmol), Co-ZIF-9 (0.8 μmol, activated), solvent (5 mL, acetonitrile/H_2O = 4:1), TEOA (1 mL), CO_2 (1 atm), $\lambda \geq 420$ nm, 20 °C, 30 min. [b] Turnover number = mol(H_2+CO)/mol(Co^{2+}). [c] In the dark. [d] Not detectable. [e] Without $[Ru(bpy)_3]Cl_2 \cdot 6H_2O$. [f] Without TEOA. [g] Without Co-ZIF-9. See the detailed description in the text for [h]–[k].

When the system was operated in absence of Co-ZIF-9, CO and H_2 production were hindered dramatically (Table 1, entry 5). We also examined the promotional effect of the ligand and Co^{2+} in a homogeneous system. Results revealed that the physical mixture of them can cocatalyze CO and H_2 evolution (entry 6), but with lower rates than those with Co-ZIF-9. This data is a strong indication that the Co-ZIF-9 solid remarkably promotes the photochemical reaction, even as a heterogeneous cocatalyst.

To further validate the critical role of the formation of metal–organic networks in supporting photocatalysis, the Co-ZIF-9 was destroyed by calcination at 1200 °C in He gas and the residues were applied in the system (Table 1, entry 7): the total generation of CO and H_2 was found to decrease sharply, thus demonstrating the vital role of the framework of Co-ZIF-9 in the CO_2 splitting by the promotion of carrier transfer and substrate concentration.

The participation of CO_2 in the reaction was also investigated by replacing CO_2 with N_2 (Table 1, entry 8). After 30 minutes of reaction, only 1.0 μmol H_2 was detected under the same reaction conditions, without any CO generated. Evidently, in the absence of CO_2, light-induced electrons can promote H_2 generation only. However, in the presence of CO_2, the overall efficiency of the photochemical reduction process for both CO (41.8 μmol/30 min) and H_2 (29.9 μmol/30 min) production greatly increase. This result is a remarkable observation in that the capture and activation of CO_2 by the system also accelerates/activates the H_2 liberation: the CO_2-containing Co-ZIF-9 is a better hydrogen reduction catalyst, potentially by the influence of CO_2 on the water/TEOA structure on the zeolitic pores.

After the reaction, the Co-ZIF-9 was removed from the reaction mixture. Inductively-coupled plasma analysis of the resultant supernatant revealed that only 0.5% cobalt ions leak from the Co-ZIF-9. Trace amounts of formic acid (HCOOH) were produced in the supernatant as detected by ion chromatograph. The supernatant was reused for the CO_2 reduction reaction under identical reaction conditions. Results show that the system is virtually inactive (Table 1, entry 9), thus suggesting the heterogeneous nature of the current system.

To further confirm the source of the produced CO, we performed an isotopic experiment using $^{13}CO_2$. The evolution of CO was analyzed by gas chromatography mass spectrometry. After 30 minutes, the peak at 3.57 min with m/z 29 was assigned to ^{13}CO (see Figure S4). This data provides a solid proof that Co-ZIF-9 can indeed promote the deoxygenative reduction of CO_2 into CO, thus precluding the degradation effect of organics in the system.

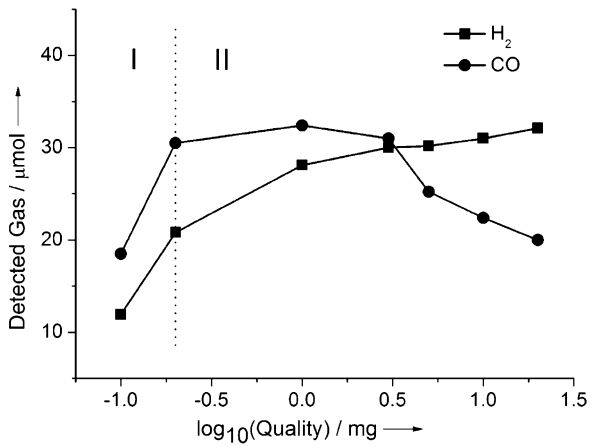

Figure 2. The effect of the amount of Co-ZIF-9 on the evolution of CO and H_2 from the CO_2 photoreduction system.

Next, we studied the effect of the amount of Co-ZIF-9 on the photochemical performance of the system (Figure 2). Obviously, the production of CO and H_2 increases substantially, even when only a tiny amount of Co-ZIF-9 (0.1 mg) added. When 1 mg Co-ZIF-9 was added to the reaction system, the activity reached a maximum value for the production of CO and H_2. Further increasing the amount of Co-ZIF-9 leads to a slight increase in H_2 generation, while the production of CO decreases slightly. Clearly, the reaction pathways for CO and H_2 production are different, but it is clear that in region I (Figure 2, cocatalyst < 0.2 mg) the reaction rate is mainly limited by the number of catalytic centers which can be accessed by the sensitizer, while in region II (cocatalyst > 0.2 mg) the reaction rate is largely determined by electron-transfer kinetics.[24] Note that the total generation of CO and H_2 stays almost unaltered in this region. Even with an excessive amount of Co-ZIF-9 added, the total production of the products did not increase, thus identifying electron transfer from the sensitizer as the rate-determining step. All these results highlight the dual functions of Co-ZIF-9 in assisting CO_2 fixation by acting as a CO_2 absorber and a redox promoter, but combined in a microporous MOF.

As described above, the as-prepared Co-ZIF-9 is already active for CO_2 reduction, but generally restricted by the blocking of micropores by guest molecules adsorbed on the surface and within the channels of MOFs. To maximize the catalytic function, the Co-ZIF-9 was activated by thermal treatment under vacuum for 4 hours to eliminate water and organic solvents trapped. The activity of Co-ZIF-9 as a function of activation temperature is shown in Figure S5. Obviously, as the activation temperature increased, the yield of CO and H_2 improved gradually, thus achieving a maximum value at 110 °C. Further increase in the temperature, led to a decrease in the yield presumably because of the damage of the framework at higher temperature in the vacuum. The apparent quantum yield of this optimized MOF-promoted CO_2 photoreduction system was estimated to be 1.48 % at monochromatic irradiation of $\lambda = 420$ nm.

The CO/H_2 generation from the activated Co-ZIF-9 catalytic system as a function of reaction time is shown in Figure S6. For the initial reaction of 30 minutes, the total amount of CO and H_2 increased dramatically, but thereafter increased slightly. We attribute this decrease to photobleaching of the dye after limited photocatalytic turnovers (TON = 7 with respect to the dye).[25] To this end, the development of a durable, cheap candidate as a light harvester is recommended.

The effect of reaction temperature was also investigated. As the reaction temperature increased, the yields of CO and H_2 increased gradually, thus reaching a maximum value at 30 and 40 °C, respectively. By additionally increasing the reaction temperature, both the production of CO and H_2 were reduced (see Figure S7).

To check the stability of Co-ZIF-9, two methods were applied, namely, 1) recovery of the used Co-ZIF-9 and then redispersion in a fresh dye solution for 0.5 hour of reaction, and 2) addition of new dye into the system after 1 hour of reaction. For both methods the material virtually kept its intrinsic catalytic activity for five repetitions of the operation. As shown in Figure 3 a, the activity of the reused catalysts has

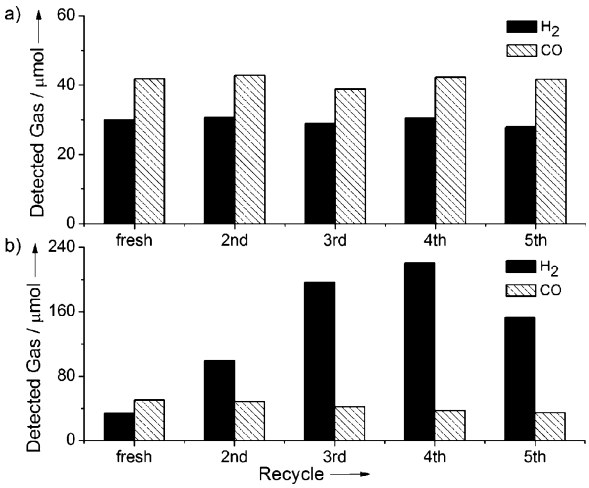

Figure 3. The stability test of Co-ZIF-9 in five repeats of photocatalytic operations. a) Recovery of the used catalyst and then redispersion in a fresh dye solution for 0.5 h reaction. b) Addition of the new dye into the system after 1 h reaction.

no noticeable alteration. The total production of the reaction products was calculated to be about 350 μmol, thus corresponding to a catalytic TON of about 450 in 2.5 hours. However, in another set of stability tests, wherein the new dye was added into the system after 1 hour of reaction, the evolution of H_2 gradually increased in the first 4 runs, but the CO production decreased (Figure 3 b). This decrease can be explained by the formation of a ruthenium species as a H_2-evoltuion catalyst from the degradation of the ruthenium dye. In the final run, both H_2 and CO production decreased after adding an excessive amount of dye, because of the light-shielding effect.

After the reaction, there is no noticeable change in the chemical, crystal, and surface structures of the Co-ZIF-9

sample (see Figures S8–10). These results reflect the stable characteristics of the MOF in the photoredox chemistry system.

The wavelength dependence of the CO and H_2 production revealed that the trend of CO and H_2 evolution matched well with the optical absorption of the dye molecule (see Figure S11) instead of that of Co-ZIF-9. This research confirmed that the reaction was indeed induced by light excitation of the dye, thus ruling out the contribution of the metal-to-ligand charge transfer in Co-ZIF-9.

Table 2: Comparison of cocatalytic functions of Co-ZIF-9[a] with other MOFs and cobalt complex.[b]

MOFs	CO [μmol]	H_2 [μmol]	TON
Co-MOF-74	11.7	7.3	23.8
Mn-MOF-74	1.5	2.9	5.5
Zn-ZIF-8	2.1	2.4	5.6
Zr-UiO-66-NH_2	1.2	2.2	4.3
$C_{10}H_{10}Co$	5.0	2.7	9.6

[a] The activity data of Co-ZIF-9 was provided in the entry 1 of Table 1. [b] Reaction conditions are the same as those in Table 1.

Some other MOFs were also applied as cocatalysts in the system to explore the uniqueness of Co-ZIF-9 in promoting CO_2 reduction catalysis (Table 2). Once Co-ZIF-9 was replaced by Co-MOF-74 (ligand: 2,5-dihydroxyterephthalic acid), the production of both CO and H_2 decreased greatly. This result is a strong indication that the imidazolate-based ligand plays a key role in capture of CO_2 because of the high chemical affinity of benzimidazolate motifs to CO_2. When Mn-MOF-74 (ligand: 2,5-dihydroxyterephthalic acid) was applied, the system catalyzes CO and H_2 production, but only with a slight improvement over the cocatalyst-free system (Table 1, entry 5). This observation however provides vital proof that the electron-mediating functions of cobalt species are indispensable for supporting CO_2 conversion. As expected, when either Zn-ZIF-8 (ligand: 2-methylimidazole) or Zr-UiO-66-NH_2 (ligand: NH_2-1,4-benzenedicarboxylic acid) was used, there is no obvious CO_2 reduction. Cobaltocene was also used as a homogeneous cocatalyst in the reaction, and there was only a tiny enhancement in yield of CO and H_2, again underlining the synergetic effect of cobalt and benzimidazolate entities for CO_2 conversion.

In conclusion, we have presented an example of MOFs based on cobalt clusters and benzimidazolate motifs as stable cocatalysts for supporting the photocatalytic splitting of CO_2 into CO under mild reaction conditions by merging the advantage of porous characteristic of the MOF, for CO_2 capture, together with the catalytic function of imidazolate entities and cobalt in CO_2 reduction catalysis. These findings will open up new opportunities in artificial photosynthesis by assembling various catalytically active metals, functional organic ligands, and antenna complexes onto or into porous MOF materials.

Received: October 29, 2013
Published online: December 11, 2013

Keywords: carbon dioxide · cobalt · metal–organic frameworks · photochemistry · zeolites

[1] a) T. Sakakura, J. C. Choi, H. Yasuda, *Chem. Rev.* **2007**, *107*, 2365 – 2387; b) K. R. Thampi, J. Kiwi, M. Gratzel, *Nature* **1987**, *327*, 506 – 508; c) E. Greenbaum, J. W. Lee, C. V. Tevault, S. L. Blankinship, L. J. Mets, *Nature* **1995**, *376*, 438 – 441; d) W. C. Chueh, C. Falter, M. Abbott, D. Scipio, P. Furler, S. M. Haile, A. Steinfeld, *Science* **2010**, *330*, 1797 – 1801; e) H. Arakawa, et al., *Chem. Rev.* **2001**, *101*, 953 – 996.

[2] a) J. M. Lehn, R. Ziessel, *Proc. Natl. Acad. Sci. USA* **1982**, *79*, 701 – 704; b) J. Ettedgui, Y. Diskin-Posner, L. Weiner, R. Neumann, *J. Am. Chem. Soc.* **2010**, *132*, 188 – 190; c) Y. Matsumoto, M. Obata, J. Hombo, *J. Phys. Chem.* **1994**, *98*, 2950 – 2951; d) K. Maeda, K. Sekizawa, O. Ishitani, *Chem. Commun.* **2013**, *49*, 10127 – 10129.

[3] A. J. Morris, G. J. Meyer, E. Fujita, *Acc. Chem. Res.* **2009**, *42*, 1983 – 1994.

[4] a) Z. Qin, C. M. Thomas, S. Lee, G. W. Coates, *Angew. Chem.* **2003**, *115*, 5642 – 5645; *Angew. Chem. Int. Ed.* **2003**, *42*, 5484 – 5487; b) C. T. Cohen, T. Chu, G. W. Coates, *J. Am. Chem. Soc.* **2005**, *127*, 10869 – 10878; c) J. Louie, J. E. Gibby, M. V. Farnworth, T. N. Tekavec, *J. Am. Chem. Soc.* **2002**, *124*, 15188 – 15189.

[5] a) C. M. Mömming, E. Otten, G. Kehr, R. Fröhlich, S. Grimme, D. W. Stephan, G. Erker, *Angew. Chem.* **2009**, *121*, 6770 – 6773; *Angew. Chem. Int. Ed.* **2009**, *48*, 6643 – 6646; b) E. R. Pérez, R. H. A. Santos, M. T. P. Gambardella, L. G. M. de Macedo, U. P. Rodrigues-Filho, J. C. Launay, D. W. Franco, *J. Org. Chem.* **2004**, *69*, 8005 – 8011; c) A. E. Ashley, A. L. Thompson, D. O'Hare, *Angew. Chem.* **2009**, *121*, 10023 – 10027; *Angew. Chem. Int. Ed.* **2009**, *48*, 9839 – 9843.

[6] a) P. Wasserscheid, *Nature* **2006**, *439*, 797 – 797; b) R. D. Rogers, K. R. Seddon, *Science* **2003**, *302*, 792 – 793; c) T. Welton, *Chem. Rev.* **1999**, *99*, 2071 – 2084.

[7] a) E. D. Bates, R. D. Mayton, I. Ntai, J. H. Davis, *J. Am. Chem. Soc.* **2002**, *124*, 926 – 927; b) C. Wang, H. Luo, D. Jiang, H. Li, S. Dai, *Angew. Chem.* **2010**, *122*, 6114 – 6117; *Angew. Chem. Int. Ed.* **2010**, *49*, 5978 – 5981.

[8] a) B. A. Rosen, A. Salehi-Khojin, M. R. Thorson, W. Zhu, D. T. Whipple, P. J. A. Kenis, R. I. Masel, *Science* **2011**, *334*, 643 – 644; b) H. A. Schwarz, R. W. Dodson, *J. Phys. Chem.* **1989**, *93*, 409 – 414; c) B. A. Rosen, J. L. Haan, P. Mukherjee, B. Braunschweig, W. Zhu, A. Salehi-Khojin, D. D. Dlott, R. I. Masel, *J. Phys. Chem. C* **2012**, *116*, 15307 – 15312.

[9] a) N. E. Kamber, W. Jeong, R. M. Waymouth, R. C. Pratt, B. G. G. Lohmeijer, J. L. Hedrick, *Chem. Rev.* **2007**, *107*, 5813 – 5840; b) D. P. Curran, A. Solovyev, B. M. Makhlouf, L. Fensterbank, M. Malacria, E. Lacôte, *Angew. Chem.* **2011**, *123*, 10476 – 10500; *Angew. Chem. Int. Ed.* **2011**, *50*, 10294 – 10317.

[10] a) D. Yu, Y. Zhang, *Proc. Natl. Acad. Sci. USA* **2010**, *107*, 20184 – 20189; b) H. Zhou, W. Z. Zhang, C. H. Liu, J. P. Qu, X. B. Lu, *J. Org. Chem.* **2008**, *73*, 8039 – 8044; c) S. N. Riduan, Y. Zhang, J. Y. Ying, *Angew. Chem.* **2009**, *121*, 3372 – 3375; *Angew. Chem. Int. Ed.* **2009**, *48*, 3322 – 3325.

[11] a) O. K. Farha, J. T. Hupp, *Acc. Chem. Res.* **2010**, *43*, 1166 – 1175; b) S. L. James, *Chem. Soc. Rev.* **2003**, *32*, 276 – 288; c) A. I. Cooper, M. J. Rosseinsky, *Nat. Chem.* **2009**, *1*, 26 – 27.

[12] a) N. L. Rosi, J. Eckert, M. Eddaoudi, D. T. Vodak, J. Kim, M. O'Keeffe, O. M. Yaghi, *Science* **2003**, *300*, 1127 – 1129; b) S. Ma, H. C. Zhou, *J. Am. Chem. Soc.* **2006**, *128*, 11734 – 11735; c) S. T. Zheng, J. T. Bu, Y. Li, T. Wu, F. Zuo, P. Feng, X. Bu, *J. Am. Chem. Soc.* **2010**, *132*, 17062 – 17064.

[13] a) E. D. Bloch, W. L. Queen, R. Krishna, J. M. Zadrozny, C. M. Brown, J. R. Long, *Science* **2012**, *335*, 1606 – 1610; b) Y. He, S. Xiang, B. Chen, *J. Am. Chem. Soc.* **2011**, *133*, 14570 – 14573; c) N.

Nijem, H. Wu, P. Canepa, A. Marti, K. J. Balkus, T. Thonhauser, J. Li, Y. J. Chabal, *J. Am. Chem. Soc.* **2012**, *134*, 15201 – 15204.
[14] a) P. Wu, C. He, J. Wang, X. Peng, X. Li, Y. An, C. Duan, *J. Am. Chem. Soc.* **2012**, *134*, 14991 – 14999; b) L. Ma, J. M. Falkowski, C. Abney, W. Lin, *Nat. Chem.* **2010**, *2*, 838 – 846; c) X. L. Yang, M. H. Xie, C. Zou, Y. He, B. Chen, M. O'Keeffe, C. D. Wu, *J. Am. Chem. Soc.* **2012**, *134*, 10638 – 10645; d) M. Dan-Hardi, C. Serre, T. Frot, L. Rozes, G. Maurin, C. Sanchez, G. Férey, *J. Am. Chem. Soc.* **2009**, *131*, 10857 – 10859.
[15] a) Z. Xie, L. Ma, K. E. DeKrafft, A. Jin, W. Lin, *J. Am. Chem. Soc.* **2009**, *131*, 922 – 923; b) B. Chen, L. Wang, Y. Xiao, F. R. Fronczek, M. Xue, Y. Cui, G. Qian, *Angew. Chem.* **2009**, *121*, 508 – 511; *Angew. Chem. Int. Ed.* **2009**, *48*, 500 – 503.
[16] a) K. S. Min, M. P. Suh, *J. Am. Chem. Soc.* **2000**, *122*, 6834 – 6840; b) M. Kim, J. F. Cahill, H. Fei, K. A. Prather, S. M. Cohen, *J. Am. Chem. Soc.* **2012**, *134*, 18082 – 18088.
[17] a) P. Horcajada, C. Serre, M. Vallet-Regí, M. Sebban, F. Taulelle, G. Férey, *Angew. Chem.* **2006**, *118*, 6120 – 6124; *Angew. Chem. Int. Ed.* **2006**, *45*, 5974 – 5978; b) J. An, S. J. Geib, N. L. Rosi, *J. Am. Chem. Soc.* **2009**, *131*, 8376 – 8377.
[18] a) H. Hayashi, A. P. Cote, H. Furukawa, M. O'Keeffe, O. M. Yaghi, *Nat. Mater.* **2007**, *6*, 501 – 506; b) J. P. Zhang, Y. B. Zhang, J. B. Lin, X. M. Chen, *Chem. Rev.* **2011**, *111*, 1001 – 1033.
[19] K. S. Park, Z. Ni, A. P. Côté, J. Y. Choi, R. Huang, F. J. Uribe-Romo, H. K. Chae, M. O'Keeffe, O. M. Yaghi, *Proc. Natl. Acad. Sci. USA* **2006**, *103*, 10186 – 10191.
[20] a) R. Banerjee, A. Phan, B. Wang, C. Knobler, H. Furukawa, M. O'Keeffe, O. M. Yaghi, *Science* **2008**, *319*, 939 – 943; b) B. Wang, A. P. Cote, H. Furukawa, M. O'Keeffe, O. M. Yaghi, *Nature* **2008**, *453*, 207 – 211; c) C. M. Miralda, E. E. Macias, M. Zhu, P. Ratnasamy, M. A. Carreon, *ACS Catal.* **2011**, *1*, 180 – 183.
[21] a) O. Karagiaridi, M. B. Lalonde, W. Bury, A. A. Sarjeant, O. K. Farha, J. T. Hupp, *J. Am. Chem. Soc.* **2012**, *134*, 18790 – 18796; b) M. B. Lalonde, O. K. Farha, K. A. Scheidt, J. T. Hupp, *ACS Catal.* **2012**, *2*, 1550 – 1554.
[22] L. T. L. Nguyen, K. K. A. Le, H. X. Truong, N. T. S. Phan, *Catal. Sci. Technol.* **2012**, *2*, 521 – 528.
[23] P. L. Spath, N. D. C. Dayton, *National Renewable Energy Laboratory: Golden*, *CO*, **2003**, REL/TP-510 – 34929.
[24] T. Maschmeyer, M. Che, *Angew. Chem.* **2010**, *122*, 1578 – 1582; *Angew. Chem. Int. Ed.* **2010**, *49*, 1536 – 1539.
[25] a) R. Ziessel, J. Hawecker, J. M. Lehn, *Helv. Chim. Acta* **1986**, *69*, 1065 – 1084; b) J. M. Lehn, R. Ziessel, *J. Organomet. Chem.* **1990**, *382*, 157 – 173.

